Spectrochimica Acta Part A: Molecular and Biomolecular Spectroscopy 157 (2016) 96–103

Contents lists available at ScienceDirect

Spectrochimica Acta Part A: Molecular and Biomolecular Spectroscopy

journal homepage: www.elsevier.com/locate/saa

Synthesis and spectral characterization of bis(4-amino-5-mercapto-1,2,4-triazol-3-yl)propane

S. Subashchandrabose [a], V. Thanikachalam [b], G. Manikandan [b], H. Saleem [c,*], Y. Erdogdu [d]

[a] Centre for Research and Development, PRIST University, Thanjavur, Tamil Nadu, 613403, India
[b] Dept. of Chemistry, Annamalai University, Annamalai Nagar, Tamil Nadu 608 002, India
[c] Dept. of Physics, Annamalai University, Annamalai Nagar, Tamil Nadu 608 002, India
[d] Dept. of Physics, Ahi Evran University, 40040, Kirsehir, Turkey

ARTICLE INFO

Article history:
Received 27 November 2014
Received in revised form 20 November 2015
Accepted 5 December 2015
Available online 8 December 2015

Keywords:
MOT
FT-IR
FT-Raman
DFT
NBO

ABSTRACT

Bis(4-amino-5-mercapto-1,2,4-triazol-3-yl)propane (BAMTP) was synthesized and characterized by FT-IR and FT-Raman spectra. Gas phase structure of BAMTP was examined under density functional theory B3LYP/6-311++G(d, p) level of basis set, wherein the molecule was subjected to conformational analysis. Thus the identified stable structure utilized for the calculations such as geometry optimization, vibrational behavior, hyperpolarizability analysis, natural bond orbital analysis, band gap, chemical hard/softness and stability. Geometry of BAMTP has been discussed elaborately with related crystal data. The results found from experimental and theoretical methods were reported herewith.

1. Introduction

Organic molecules play an important role in solar cell applications due to their excellent optical and electrical properties [1–3]. Nitrogen containing heterocyclic molecules such as pyrazole, imidazole, triazole, pyridine, pyrimidine and pyrazine was used as an additive in dye sensitized solar cells [4]. Since triazole contains more nitrogen, the dendrimers of triazole were considered to improve the efficiency in solar cell devices [5]. Recent reports reveal the application of 1,2,3-triazole and 1,2,4-triazole dendrimers as additives in redox couple for dye-sensitized solar cells [6,7]. In addition to that the most effective corrosion inhibitors are those compounds containing hetero-atoms like nitrogen, oxygen, sulfur and phosphorus [8–11]. Most of the nitrogen-containing molecules are pharmacologically active especially the triazole representing a very interesting class of compounds because of their wide applications in analytical, industrial and pharmaceutical applications [12–18]. In recent years, triazole-based chemosensory molecules have also been investigated and shown to be successfully applicable in biological systems [19]. Since the biological action mainly depends on stereochemistry of the molecule, it is important to study the conformation of molecule. Based on the above factors, in the present paper, we report synthesis of bis(4-amino-5-mercapto-1,2,4-triazol-3-yl)propane (BAMTP) structural conformation, vibrational behavior, nonlinear optical properties (NLO), hybridization, energy gap (E_g) and hard/softness, using FT-IR, FT-Raman spectra and density functional theory (DFT) calculations. This paper also dealt with the bond order, sigma (σ) and pi (π) electron appearance, percentage of electron densities at *s*-orbital and *p*-orbital, and scope of electron at *d*-orbital.

2. Experimental details

The FT-Raman spectrum of BAMTP has been recorded using 1064 nm line of Nd: YAG laser as excitation wavelength in the region 50–3500 cm^{-1} on a Thermo Electron Corporation model Nexus 670 spectrophotometer equipped with FT-Raman module accessory. The FT-IR spectrum of this compound was recorded in the range of 400–4000 cm^{-1} on Nexus 670 spectrophotometer using KBr pellet technique, at room temperature, with scanning speed of 30 cm^{-1}/min and the spectral resolution of 4.0 cm^{-1}. The spectral measurements were carried out from the Central Electro Chemical Research Institute [CECRI], Karaikudi, Tamil Nadu.

2.1. Synthesis of bis(4-amino-5-mercapto-1, 2, 4-triazol-3-yl)propane

A mixture of glutaric acid (0.01 mol) and thiocarbohydrazide (0.02 mol) was warmed carefully until melting occurred and then it was stirred at 170 °C for 30 min. The reaction mixture was then cooled to room temperature and mixed with water (50 ml). The precipitate was filtered off, washed with water and 95% ethanol and finally recrystallized from DMSO.

* Corresponding author.
E-mail address: saleem_h2001@yahoo.com (H. Saleem).

http://dx.doi.org/10.1016/j.saa.2015.12.005
1386-1425/

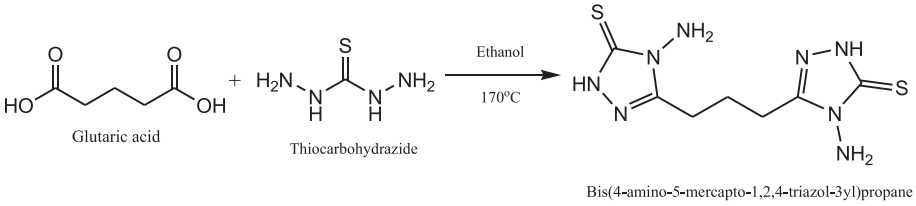

3. Computational details

The entire calculations were performed at DFT levels on a Pentium IV/3.02 GHz personal computer using *Gaussian* 03W [20–22] program package, invoking gradient geometry optimization [21]. The optimized structural parameters were used in the vibrational frequency calculations at the DFT levels to characterize all stationary points as minima. Then the vibrationally averaged nuclear positions of BAMTP were used for harmonic vibrational frequency calculations resulting in IR and Raman frequencies together with intensities. In this study, the DFT approach (B3LYP/6-311++G(d,p)) has been utilized for the computation of molecular structure.

3.1. Raman intensity prediction

It should be noted that Gaussian 03 package does not calculate the Raman intensities. The Raman activities were transformed into Raman intensities using Raint program [23] by the expression:

$$I_i = 10^{-12} \times (\nu_0 - \nu_i)^4 \times \frac{1}{\nu_i} \times RA_i \quad (1)$$

where I_i is the Raman intensity, RA_i is the Raman scattering activities, ν_i is the wavenumber of the normal modes and ν_0 denotes the wavenumber of the excitation laser [24].

4. Result and discussion

4.1. Conformational stability

A molecule can have more numbers of conformers but they may not be a stable conformer or structure. Our aim is to study the properties of ground state structure of title compound. In order to bring the stable structure, the dihedral angle C1-C7-C10-H11 of BAMTP was rotating at 20° interval up to 360° using B3LYP/6-311++G(d,p) level of basis set calculation, in which seventeen conformers were possibly obtained. To find the stable structure among the seventeen, their zero point energies were corrected with total energies. As a result, zero energy difference was obtained for conformer one and it was considered as stable one. The optimized structures and conformers are shown in Fig. 1a and b; detailed energies of all conformers are listed in Table 1.

4.2. Optimized bond parameters

BAMTP molecule belongs to C_1 point group symmetry. In BAMTP, two triazole rings are fused by propane linker. Also the sulfur (S) atom and amino group ($-NH_2$) influence the geometry of the molecule.

In a molecule the electronic configuration of an atom plays an important role in its molecular property. The electronic configuration of sulfur at the ground state is $3s^2\ 3p_x^2\ 3p_y^1\ 3p_z^1\ 3d^0$ (n = 2), at the first excited state is $3s^2\ 3p_x^1\ 3p_y^1\ 3p_z^1\ 3d^1$ (n = 4) and at the second excited state is $3s^1\ 3p_x^1\ 3p_y^1\ 3p_z^1\ 3d^1\ 3d^1$ (n = 6) [25]. In the present molecule, the sulfur atom (C═S) has two unpaired electrons at the ground state with σ and π-orbitals. The σ-bonds are stronger and elongated the bond length whereas π-bonds are weaker and shorter. The bond length of C═S in two triazole rings lies at 1.667 Å; it falls in the range of σ orbitals (C–S). Whereas, bond lengths of each C═N in BAMTP have shown to be 1.3 Å; it is due to the overlap of π orbitals (C═N). In the geometry of NH_2 groups at triazole rings, the nitrogen atom in ground state is $2s^2\ 2p_x^1\ 2p_y^1\ 2p_z^1$ configuration; it has sp^3 hybridization and their bond lengths lie at 1.019 Å in both rings due to the lower inter nuclear distance between 1s and 2p orbitals [25]. The rest of the bond parameters of this molecule are listed in Table 2.

4.3. Vibrational spectral analysis

This molecule consists of 29 atoms, and hence 81 normal modes are possible. The 81 normal vibrations are distributed as $26A_1 + 15A_2 + 16B_1 + 24B_2$ where A_1, B_1 and B_2 are active in both IR and Raman and A_2 is active in Raman. The calculated frequencies together with the experimental data of BAMTP molecule are presented in Table 3. Theoretical and experimental spectra of BAMTP are given in Figs. 2 and 3. The total energy distribution (TED) was calculated by using the SQM software [26,27] and the vibrational modes were characterized by their TED.

In general, the differences between the observed and predicted frequencies are small for most of the fundamental vibrations. Some of the discrepancies are due to the approximate nature of the method used in the calculations. Some others are due to the intermolecular interactions that occur in the chemical environmental. Based on the comparison of the calculated and experimental spectra, the band assignment was performed.

4.3.1. CH_2 vibrations

The fundamental CH_2 vibrations are able to scissor, wag, twist and rock in the expected frequency region 1500–800 cm^{-1} [28]. The calculated CH_2 symmetric stretching vibrations appear at 2946, 2927 and 2925 cm^{-1} (mode nos: 12–10) by B3LYP/6-311++G(d, p) level. Serbest et al. [29] have recorded the asymmetric mode of methylene group at 2969 cm^{-1}, 2988 cm^{-1} and 2909 cm^{-1}. In the present investigation, the CH_2 symmetric and asymmetric vibrations are observed at 2772 cm^{-1} (FT-IR), 2909 cm^{-1} (FT-Raman) and 2948 cm^{-1}, 3053 cm^{-1} (FT-IR), and 2988 cm^{-1} (FT-Raman) respectively. The computed ν_{asy} CH_2 modes are at 2948 cm^{-1}, 2966 cm^{-1} and 3004 cm^{-1} (B3LYP: mode nos: (9–7) using B3LYP/6-311++G(d, p) basis set. These calculated frequencies are in good agreement with the observed and literature values.

The in-plane bending vibration of C–H appears at 1212 cm^{-1} [30]. The weak bands observed at 1362 cm^{-1} and 1050 cm^{-1} in FT-IR are attributed to δ_{C-H} mode. The theoretical δ_{C-H} mode has calculated as 1365 cm^{-1}, 1283 cm^{-1}, 1254 cm^{-1}, 1149 cm^{-1} and 1051 cm^{-1} (mode nos: 24, 29, 31, 36 and 40). These assignments are in line with experimental values. The computed δ_{CH2} modes are assigned in the range of 1414, 1431, 1433 and 1455 cm^{-1} (DFT-mode nos: 23, 21, 20 and 17). The observed bands 1492 (FT-IR) and 1429 and 1494 cm^{-1} (FT-Raman) are in agreement with theoretical values. Experimentally observed CH_2 wagging frequency appears at 1362 cm^{-1} in FT-IR spectrum; it is found to be satisfactorily in agreement with the literature [31] and calculated values (1365, 1149 cm^{-1}/B3LYP: mode nos: 24, 36). Tasal et al. [32] assigned the CH_2 twisting and rocking modes in the range of 1096–1297 and 875–763 cm^{-1}, respectively for 3-(piperidine-1-yl-methyl)-1,3-benzoxazol-2(3H)-one molecule. The

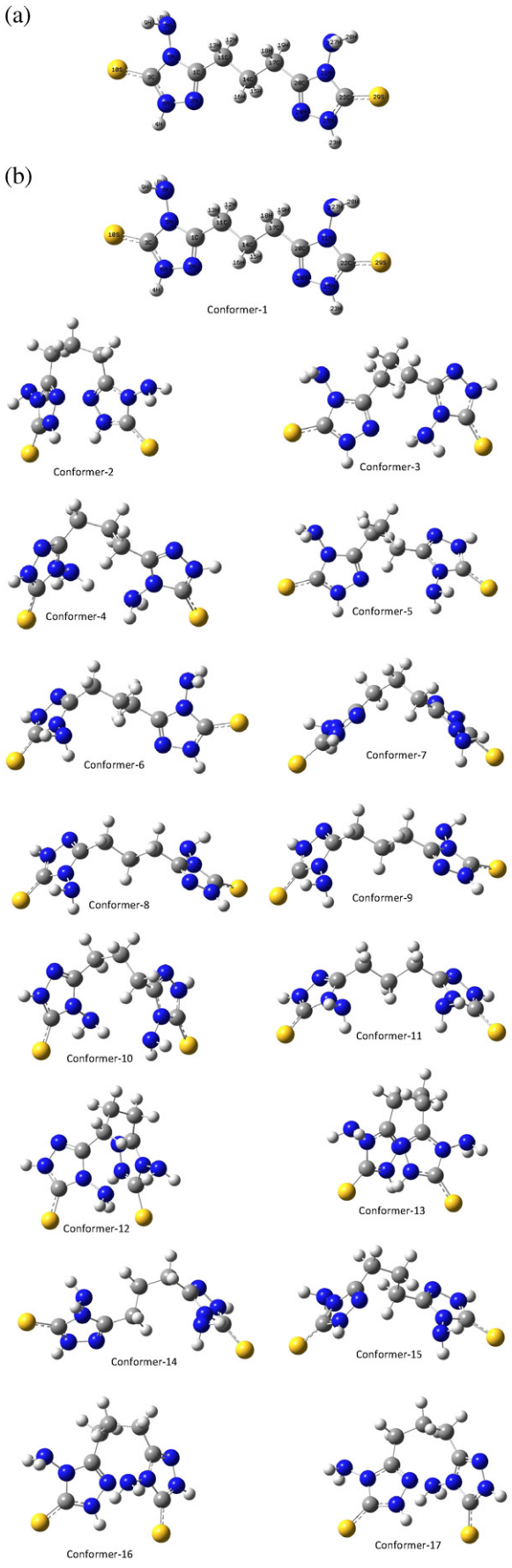

Fig. 1. (a) The optimized molecular structure of BAMTP (b) The possible conformers of BAMTP.

bands at 1050(FT-IR), 1051, 1149 (mode nos: 40, 36) and 721 cm^{-1} and 824 cm^{-1} (mode nos: 50, 47) in BAMTP have been designated to twisting and rocking of the CH_2 group.

4.3.2. NH_2 vibrations

The amino group (NH_2) stretching vibration usually appears in the range between 3500 and 3100 cm^{-1} [33–35], whereas Karakurt et al. [36] have calculated the harmonic frequency at 3541 cm^{-1}. The calculated νN–H stretching vibrational frequency was predicted at 3548 cm^{-1} and 3549 cm^{-1} (mode nos: 2, 1) using B3LYP method. The absorption band in the region of 3230–3381 cm^{-1} is attributed to the NH_2 asymmetric stretching of the amine group of the analogous molecule [31]. The NH_2 symmetric stretching mode has been assigned at 3288 cm^{-1} [37]. In the present investigation, the FT-IR spectrum shows a strong band at 3247 cm^{-1} and a medium strong FT-Raman band at 3255 cm^{-1}. They correspond to NH_2 symmetric vibration. The asymmetric stretching also observed as medium strong band in FT-IR spectrum at 3324 cm^{-1}. The B3LYP computations give the frequency of these bands at 3340 cm^{-1} and 3399 cm^{-1} (mode nos: 6–3) for υ_{sym} NH_2 and υ_{asym} NH_2 stretching vibrations respectively. These assignments are in agreement with literature [31].

According to Socrates [38], the frequencies of amino group appeared around 3500–3300 cm^{-1} due to NH_2 stretching, 1700–1600 cm^{-1} to the scissoring vibration and 1150–900 cm^{-1} appeared for rocking deformations. The internal deformation vibration known as, NH_2 scissoring frequency was observed at 1701 cm^{-1} and 1612 cm^{-1} in FT-IR spectrum, which is supported by TED and literature. The NH_2 scissoring vibration calculated 1652 cm^{-1} by B3LYP (mode no: 14) method deviates positively by 40 cm^{-1} compared to the experimental FT-IR data. The computed NH_2 twisting frequency was assigned at 1313 cm^{-1}, 1232 cm^{-1} by B3LYP method (mode nos: 26, 27 and 32). However the observed FT-IR (1317 cm^{-1}, 1234 cm^{-1} and FT-Raman (1302 cm^{-1}) bands do support the harmonic data. The NH_2 rocking computed at 935 cm^{-1} and 927 cm^{-1} by B3LYP (mode nos: 45, 46) method coincides satisfactorily with the recorded spectral values (FT-IR: 916 and Raman: 890 cm^{-1}). It should be emphasized that the wave numbers calculated by B3LYP method at 649 cm^{-1}/649 cm^{-1} (mode nos: 54, 53) for NH_2 wagging mode are supported by TED value (12%), whereas, this type of vibration is not supported by experimental data. In this study, the theoretically calculated δ_{N-H} (1443 cm^{-1}/mode no: 19) and ΓN–H (488 cm^{-1}, 486 cm^{-1}/mode nos: 59, 60) modes have been found to be consistent with recorded FT-Raman values (488, 472 cm^{-1}).

4.3.3. C–N, C═N vibrations

Literature survey reveals that the C–N and C═N stretching vibrations appeared at 1227 cm^{-1} and 1572 cm^{-1}, respectively in the case of bis(4-amino-5-mercapto-1,2,4-triazol-3-yl) ethane [37]. In the present work, the bands at 1234 cm^{-1} (weak) and 1420 cm^{-1} (strong) in FT-IR have been assigned to C–N stretching. The bands observed at 1572 cm^{-1} (strong) and 1576 cm^{-1} (medium strong) are in FT-IR and FT-Raman respectively, have been assigned to C═N stretching vibration. The identification of C–N and C═N vibrations is a very difficult task since the mixing of several bands is possible in the region. In benzotriazole, the C–N stretching bands are found to be present at 1307 cm^{-1} and 1382 cm^{-1} [39]. The theoretically scaled values of C═N vibration fall at 1566 cm^{-1} and 1571 cm^{-1} (B3LYP/mode nos: 16, 15) in both rings of the BAMTP molecule. Similarly the vibrations falling at 1416 cm^{-1}, 1414 cm^{-1}, 1287 cm^{-1}, 1261 cm^{-1}, 1232 cm^{-1}, 1223 cm^{-1} and 1217 cm^{-1} (mode nos: 22, 23, 28, 30, 32–34) are due to C–N stretching [39].

4.3.4. C═S vibrations

Identification of C═S stretching vibration is difficult and also uncertain, since the absorption of C–O and C–N also occurs in the same region. The C═S group is less polar than the C═O group and has a considerably

Table 1
Energetics of the conformers calculated at the B3LYP/6-311++G(d, p) level.

Conformers	E (Hartree)	ΔE (kcal/mol)	E_0 (Hartree)	ΔE_0 (kcal/mol)
Conformer-1	−1508.3334272	0.0000	−1508.1076690	0.0000
Conformer-2	−1508.3327255	0.4404	−1508.1071400	0.3320
Conformer-3	−1508.3318899	0.9647	−1508.1062770	0.8735
Conformer-4	−1508.3317299	1.0651	−1508.1059540	1.0762
Conformer-5	−1508.3308036	1.6464	−1508.1057150	1.2262
Conformer-6	−1508.3305924	1.7789	−1508.1054680	1.3811
Conformer-7	−1508.3305878	1.7818	−1508.1056340	1.2770
Conformer-8	−1508.3304889	1.8438	−1508.1054740	1.3774
Conformer-9	−1508.3304887	1.8440	−1508.1054720	1.3786
Conformer-10	−1508.3304775	1.8509	−1508.1046920	1.8681
Conformer-11	−1508.3302558	1.9901	−1508.1052920	1.4916
Conformer-12	−1508.3301339	2.0666	−1508.1037660	2.4492
Conformer-13	−1508.3293959	2.5297	−1508.1042150	2.1674
Conformer-14	−1508.3291708	2.6710	−1508.1040590	2.2653
Conformer-15	−1508.3291136	2.7068	−1508.1040500	2.2710
Conformer-16	−1508.3279154	3.4587	−1508.1025300	3.2248
Conformer-17	−1508.3271729	3.9246	−1508.1021280	3.4770

E_0. Zero point corrected energy.

weak band. The compounds that contain a thiocarbonyl group show absorption in the region 1020–1250 cm^{-1} [40]. In nitrogen containing thiocarbonyl compounds, the assignment of C═S stretching frequency has been a controversial one [41,42], thus, only the results from TED can provide the clear cut assignment for the C═S vibration. In BAMTE (Ethane), the C═S stretching frequency is assigned to 1189 cm^{-1} [37]. In our present study, the C═S stretching vibrations calculated to be 1155 cm^{-1}, 1144 cm^{-1} (B3LYP/mode nos: 35, 37) are in agreement with the recorded values of 1187 cm^{-1} in FT-Raman and 1137 cm^{-1} in FT-IR, respectively. These assignments are supported by TED (12%). According to the calculated frequencies by B3LYP method, the C═S in-plane and out-of-plane bending vibrations contribute to the band at 608 cm^{-1} (mode no: 57) and 144 cm^{-1} and 123 cm^{-1} (mode nos: 74 and 75), respectively, which is in agreement with the Raman bands (611 and 151 cm^{-1}). The harmonic (B3LYP)/observed bands at 251 cm^{-1}, 224 cm^{-1} (mode nos: 67, 68)/236, 229 cm^{-1} and 144, 123 cm^{-1} (mode nos: 74, 75)/151 cm^{-1} have been designated to $\delta_{N-C=S}$ and $\Gamma_{N-C=S}$ respectively.

Table 2
The optimized bond parameters of BAMTP using B3LYP/6-311++G(d, p) level.

Parameters	Bond lengths	Parameters	Bond angles (°)
C1–N2	1.300	N5–N7–H9	107.64
C1–N5	1.383	H8–N7–H9	106.12
C1–C11	1.492	C1–C11–H12	108.24
N2–N6	1.376	C1–C11–H13	108.24
C3–N5	1.390	C1–C11–C14	113.29
C3–N6	1.355	H12–C11–H13	105.27
C3–S10	1.667	H12–C11–C14	110.72
H4–N6	1.007	H13–C11–C14	110.72
N5–N7	1.395	C11–C14–H15	109.99
N7–H8	1.019	C11–C14–H16	109.99
N7–H9	1.019	C11–C14–C17	110.83
C11–H12	1.096	H15–C14–H16	105.93
C11–H13	1.096	H15–C14–C17	109.99
C11–C14	1.532	H16–C14–C17	109.99
C14–H15	1.092	C14–C17–H18	110.72
C14–H16	1.092	C14–C17–H19	110.72
C14–C17	1.532	C14–C17–C20	113.29
C17–H18	1.096	H18–C17–H19	105.27
C17–H19	1.096	H18–C17–C20	108.24
C17–C20	1.492	H19–C17–C20	108.24
C20–N21	1.383	C17–C20–N21	123.39
C20–N24	1.300	C17–C20–N24	126.32
N21–C22	1.390	N21–C20–N24	110.29
N21–N26	1.395	C20–N21–C22	109.29
C22–N25	1.355	C20–N21–N26	124.81
C22–S29	1.667	C22–N21–N26	125.90
H23–N25	1.007	N21–C22–N25	101.50
N24–N25	1.376	N21–C22–S29	127.63
N26–H27	1.019	N25–C22–S29	130.88
N26–H28	1.019	C20–N24–N25	104.55
Bond angles (°)		C22–N25–H23	125.32
N2–C1–N5	110.29	C22–N25–N24	114.38
N2–C1–C11	126.32	H23–N25–N24	120.31
N5–C1–C11	123.39	N21–N26–H27	107.64
C1–N2–N6	104.55	N21–N26–H28	107.64
N5–C3–N6	101.50	H27–N26–H28	106.12
N5–C3–S10	127.63	Dihedrals (°)	
N6–C3–S10	130.88	C1–N2–N6–C3	0.00
C1–N5–C3	109.29	C1–N2–N6–H4	180.00
C1–N5–N7	124.81	N6–C3–N5–C1	0.00
C3–N5–N7	125.90	N6–C3–N5–N7	180.00
N2–N6–C3	114.38	S10–C3–N5–C1	180.00
N2–N6–H4	120.31	S10–C3–N5–N7	0.00
C3–N6–H4	125.32	C1–N5–N7–H8	123.00
N5–N7–H8	107.64	C1–N5–N7–H9	−123.00

4.4. NBO analysis

NBO analysis provides an efficient method for studying intra-and inters molecular bonding interaction among the bonds and also provides a convenient method for investigating charge transfer or conjugative interaction in molecular systems. Some electron donor/acceptor orbital and the interacting stabilization energy that resulted from the second-order microdisturbance theory were reported [43,44]. The larger the $E^{(2)}$ value, the more intensive in the interaction between electron donors and electron acceptors *i.e.*, the more donating tendency from the electron donors to electron acceptors and the greater the extent of conjugation of the whole system. Delocalization of electron density occupied between Lewis-type (bond or lone pair) NBO orbitals and formally corresponds to a stabilizing donor–acceptor interaction [45]. The second order Fock matrix was carried out to evaluate the donor–acceptor interactions in the NBO basis [46]. For each donor (i) and acceptor (j), the stabilization energy $E^{(2)}$ associated with the delocalization $i \rightarrow j$ estimated as

$$E^{(2)} = \Delta E_{ij} = q_i \frac{F(i,j)^2}{\varepsilon_j - \varepsilon_i} \tag{2}$$

where q_i is the donor orbital occupancy, ε_i and ε_j are diagonal elements and $F(i,j)$ is the off diagonal NBO Fock matrix element. In this investigation, the NBO analysis provides the intra-molecular charge transfer within the molecule. From Tables 4 and 5, the charge transfer between LPN5 and C_1–N_2, C_3–S_{10} is about 43.82 and 60.99 kJ/mol, respectively. The larger the $E^{(2)}$ energy, affect the length of donor bonds. It is evidenced from NBO analysis that the n-π* transition, which yields maximum delocalization energy, whereas the corresponding bond length decreased; it is due to an increase of electron density into the bond. In addition, the sp^3 hybridization formed between the sulfur and carbon atoms, in which 1s orbital of carbon (C_3) atom possesses occupancy electron about 0.9995, 2s orbital has 0.4821; similarly, the orbitals $2p_x$, $2p_y$ and $2p_z$ have 0.4495, 0.4633 and 0.4449 respectively. The energy of these 2p orbitals in C_3 is comparatively lesser than that of 2s orbitals. On the other hand, the ground state sulfur has showed more energy than carbon atom, for the reason that its 2p (p_x, p_y and p_z) orbitals obtained approximately equal occupancy (0.9998) and are higher than 2p of carbon. The higher energy levels such as d_{xy}, d_{xz}, d_{yz}, d_{x2-y2} and d_{z2} are being vacant orbitals. To utilize these orbitals the molecule has to excite to the higher energy levels.

4.5. Energy gap (HOMO-LUMO)

The atomic orbital compositions of the frontier molecular orbitals of the title compound are shown in Fig. 4. The HOMO–LUMO energy gap of these compounds was calculated at the B3LYP/6-311++(d,p) level. The HOMO represents the ability to donate an electron; LUMO as an

Table 3
The vibrational wave numbers obtained for BAMTP by experimental and B3LYP/6-311++G(d, p) [harmonic frequency (cm^{-1}), IR, Raman Intensities (km/mol)].

Mode No.	Experimental and calculated frequencies cm^{-1}			Intensity		[d]TED %
	Species	FT-IR	FT-Raman	[a]B3LYP	[b]IR_c [c]RS_c	Vibrational assignments
1	A_1			3549	33.76 26.78	$\nu_{N6H4(50)} + \nu_{N25H23(50)}$
2	B_2		3455ms	3548	0.01 1.83	$\nu_{N6H4(50)} + \nu_{N25H23(50)}$
3	B_1	3324ms		3399	3.56 8.22	$\nu_{N7H8(25)} + \nu_{N7H9(25)} + \nu_{N26H27(25)} + \nu_{N26H28(25)}$
4	A_2			3399	0 4.27	$\nu_{N7H8(25)} + \nu_{N7H9(25)} + \nu_{N26H27(25)} + \nu_{N26H28(25)}$
5	A_1	3247s	3255ms	3340	0.04 31.42	$\nu_{N7H8(25)} + \nu_{N7H9(25)} + \nu_{N26H27(25)} + \nu_{N26H28(25)}$
6	B_2	3119vs		3340	3.66 1.59	$\nu_{N7H8(25)} + \nu_{N7H9(25)} + \nu_{N26H27(25)} + \nu_{N26H28(25)}\ \nu$
7	B_1	3053s		3004	2.31 0.9	$\nu_{C14H15(46)} + \nu_{C14H16(46)}$
8	A_1		2988vs	2966	1.2 5.55	$\nu_{C14H15(49)} + \nu_{C14H16(49)}$
9	A_2	2948vs		2948	0 0.54	$\nu_{C11H12(25)} + \nu_{C11H13(25)} + \nu_{C17H18(25)} + \nu_{C17H19(25)}$
10	B_1			2946	1.62 15.11	$\nu_{C11H12(23)} + \nu_{C11H13(23)} + \nu_{C17H18(23)} + \nu_{C17H19(23)}$
11	A_1		2909ms	2927	2.49 45.33	$\nu_{C11H12(24)} + \nu_{C11H13(24)} + \nu_{C17H18(24)} + \nu_{C17H19(24)}$
12	B_2	2772ms		2925	0 2.57	$\nu_{C11H12(25)} + \nu_{C11H13(25)} + \nu_{C17H18(25)} + \nu_{C17H19(25)}$
13	A_1	1701w		1652	0.2 0.84	$\delta_{H8N7N5(10)} + \delta_{H8N7H9(24)} + \delta_{H27N26N21(10)} + \delta_{H27N26H28(24)}$
14	B_2	1612s		1652	18.27 1.85	$\delta_{H8N7N5(10)} + \delta_{H9N7N5(10)} + \delta_{H8N7H9(24)} + \delta_{H27N26N21(10)}\ \delta_{H28N26N21(10)} + \delta_{H27N26H28(24)}$
15	A_1	1572s	1576ms	1571	6.28 19.59	$\nu_{N2C1(32)} + \nu_{N24C20(32)}$
16	B_2			1566	9.42 0.07	$\nu_{N2C1(32)} + \nu_{N24C20(32)}$
17	A_1	1492s	1494s	1455	0.75 0.99	$\delta_{H15C14H16(24)}$
18	A_1			1445	2.93 8.97	$\nu_{N6C3(12)} + \nu_{N25C22(12)}$
19	B_2			1443	100 0.01	$\nu_{N6C3(13)} + \nu_{N25C22(13)} + \delta_{N2N6H4(10)} + \delta_{H23N25N24(10)}$
20	A_1			1433	0.03 2.9	$\delta_{HCH(21)} + \Gamma_{HCCH(24)}$
21	B_2		1429ms	1431	2.74 3.64	$\delta_{HCH(18)} + \Gamma_{HCCH(12)}$
22	A_1	1420s		1416	9.66 0.21	$\nu_{N5C1(11)} + \nu_{N21C20(11)}$
23	B_2			1414	0.05 0.64	$\nu_{NC(18)} + \nu_{NN(12)} + \delta_{HCH(12)}$
24	B_2	1362w		1365	0.75 0	$\nu_{NN(12)} + \delta_{HCC(20)} + \Gamma_{HCCH(16)}$
25	A_1		1336ms	1334	0.51 0.23	$\nu_{N7N5(11)} + \nu_{N26N21(11)}$
26	B_1	1317s		1313	1.72 0.7	$\delta_{H8N7N5(25)} + \delta_{H9N7N5(25)} + \delta_{H27N26N21(25)} + \delta_{H28N26N21(25)}$
27	A_2		1302s	1313	0 0.16	$\delta_{H8N7N5(25)} + \delta_{H9N7N5(25)} + \delta_{H27N26N21(25)} + \delta_{H28N26N21(25)}$
28	B_2			1287	49.46 1.4	$\nu_{NC(14)} + \nu_{NN(18)}$
29	A_2			1283	0 1.67	$\delta_{H15C14C11(12)} + \delta_{H16C14C11(12)} + \delta_{H15C14C17(12)} + \delta_{H16C14C17(12)}$
30	A_1			1261	0.78 6.73	$\nu_{NC(16)} + NNH(12)$
31	B_1			1254	0.02 0	$\delta_{H12C11C14(10)} + \delta_{H13C11C14(10)} + \delta_{H18C17C14(10)} + \delta_{H19C17C14(10)}$
32	B_2	1234w		1232	33.17 0.06	$\nu_{NC(16)} + \delta_{NNH(14)} + \delta_{CNH(16)}$
33	A_1			1223	0.34 0.08	$\nu_{N6C3(18)} + \nu_{N25C22(18)} + \delta_{C3N6H4(10)} + \delta_{C22N25H23(10)}$
34	B_2			1217	0.03 0.12	$\nu_{N6C3(12)} + \nu_{N25C22(12)}$
35	A_1		1187w	1155	0.81 0.47	$\nu_{NC(20)} + \nu_{SC(12)}$
36	A_2			1149	0 0.06	$\delta_{HCC(60)} + \Gamma_{HCCH(32)}$
37	B_2	1137w		1144	4.78 0.22	$\nu_{NC(20)} + \nu_{SC(12)}$
38	A_1	1080w		1071	1 0.79	$\nu_{N6N2(31)} + \nu_{N25N24(31)}$
39	B_2			1065	1.19 0.62	$\nu_{N6N2(30)} + \nu_{N25N24(30)}$
40	B_1	1050w		1051	0.03 0.03	$\delta_{HCC(16)} + \Gamma_{HCCC(30)} + \Gamma_{CCCH(30)}$
41	A_1		1043w	1046	3.81 1.92	$\nu_{C14C11(13)} + \nu_{C17C14(13)}$
42	B_2			1035	10.67 0	$\nu_{C14C11(19)} + \nu_{C17C14(19)}$
43	B_2	1004w		1001	5.27 1.85	$\nu_{C14C11(22)} + \nu_{C17C14(22)}$
44	A_1		997w	991	0.07 0.2	$\nu_{C14C11(16)} + \nu_{C17C14(16)}$
45	A_1	916s		935	27.48 0.08	$\nu_{NC(20)} + \delta_{HNN(20)}$
46	B_2		890w	927	2.39 0.12	$\nu_{NC(26)} + \delta_{HNN(20)} + \delta_{NNC(10)}$
47	A_2			824	0 0.27	$\delta_{HCC(12)} + \Gamma_{HCCN(16)} + \Gamma_{HCCH(48)}$
48	A_1		785s	797	0.53 5.35	$\nu_{C11C1(12)} + \nu_{C20C17(12)}$
49	B_2	752ms		748	1.09 0.01	$\nu_{N7N5(13)} + \nu_{C11C1(11)} + \nu_{C20C17(11)} + \nu_{N26N21(13)}$
50	B_1			721	1.22 0.16	$\delta_{HCC(16)} + \Gamma_{HCCN(12)} + \Gamma_{HCCH(56)}$
51	A_1		704s	690	0.02 6.68	$\nu_{N7N5(18)} + \nu_{N26N21(18)}$
52	B_2	666w	665w	676	0.01 0.92	$\nu_{NN(14)} + \nu_{SC(18)} + \nu_{CC(20)} + \delta_{NCN(10)} + \delta_{NNC(12)}$
53	B_1			649	4.42 0	$\Gamma_{CNNC(20)} + \Gamma_{NNCN(20)} + \Gamma_{NNCN(13)}$
54	A_2			649	0 0.88	$\Gamma_{CNNC(18)} + \Gamma_{NNCN(20)} + \Gamma_{HNCN(12)}$
55	B_1	627w	631w	633	1.18 0.26	$\Gamma_{CNCN(26)} + \Gamma_{NNCN(12)}$
56	A_2			631	0 0.76	$\Gamma_{CNCN(22)} + \Gamma_{NNCN(14)}$
57	B_2		611w	608	1.6 0.43	$\delta_{NNC(16)} + \delta_{NCS(10)} + \delta_{NCC(20)} + \delta_{CCC(14)}$
58	A_1		562w	588	1.08 1.92	$\nu_{S10C3(11)} + \nu_{S29C22(11)} + \delta_{N7N5C3(10)} + \delta_{C22N21N26(10)}$
59	B_1		488s	488	22.92 0.78	$\Gamma_{H4N6C3N5(14)} + \Gamma_{H4N6C3S10(22)} + \Gamma_{H23N25C22N21(14)}\ \Gamma_{H23N25C22S29(22)}$
60	A_2	471w	472w	486	0 0.26	$\Gamma_{H4N6C3N5(14)} + \Gamma_{H4N6C3S10(22)} + \Gamma_{H23N25C22N21(14)}\ \Gamma_{H23N25C22S29(22)}$
61	A_1		464w	470	0 14.61	$\nu_{S10C3(12)} + \nu_{S29C22(12)}$
62	B_2		395w	458	2.73 0.25	$\nu_{S10C3(17)} + \nu_{S29C22(17)}$
63	B_2		349ms	361	2.08 0.38	$\delta_{C14C11C1(12)} + \delta_{C20C17C14(12)}$
64	B_1		328w	304	0 0.12	$\Gamma_{N6N2C1C11(10)} + \Gamma_{N25N24C20C17(10)}$
65	A_2		317w	297	0 0.02	$\Gamma_{N6N2C1C11(10)} + \Gamma_{N25N24C20C17(10)}$
66	A_1		287ms	291	1.69 0.17	$\delta_{C17C14C11(20)}$
67	B_2		251w	236	0.25 2.63	$\delta_{N5C3S10(16)} + \delta_{N6C3S10(12)} + \delta_{S29C22N21(16)} + \delta_{N25C22S29(12)}$
68	A_1		224ms	229	2.69 1.08	$\delta_{N5C3S10(16)} + \delta_{N6C3S10(14)} + \delta_{S29C22N21(16)} + \delta_{N25C22S29(14)}$
69	B_1		206ms	215	7.99 0.27	$\Gamma_{H8N7N5C1(15)} + \Gamma_{H9N7N5C1(15)} + \Gamma_{H27N26N21C20(15)}\ \Gamma_{H28N26N21C20(15)}$
70	A_2		199ms	214	0 0.02	$\Gamma_{H8N7N5C1(14)} + \Gamma_{H9N7N5C1(14)} + \Gamma_{H27N26N21C20(14)}\ \Gamma_{H28N26N21C20(14)}$
71	B_1		189ms	178	6.17 0.7	$\Gamma_{H8N7N5C3(13)} + \Gamma_{H9N7N5C3(13)} + H27N26N21\Gamma_{C22(13)}\ \Gamma_{H28N26N21C22(13)}$
72	A_2		180ms	174	0 0.02	$\Gamma_{H8N7N5C3(13)} + \Gamma_{H9N7N5C3(13)}\Gamma_{H27N26N21C22(13)}\ \Gamma_{H28N26N21C22(13)}$
73	A_1		173ms	150	0.01 3.56	$\nu_{NC(10)} + \nu_{CC(38)} + \delta_{NCC(14)} + \delta_{CCC(17)}$
74	A_2		151ms	144	0 0.38	$\Gamma_{NNCS(12)}$

Table 3 (*continued*)

Mode No.	Experimental and calculated frequencies cm^{-1}			Intensity		[d]TED %
	Species	FT-IR	FT-Raman	[a]B3LYP	[b]IR_c [c]RS_c	Vibrational assignments
75	B_1			123	0.56 0.01	$\Gamma_{NNCS\ (17)} + \Gamma_{CNCC(12)}$
76	B_2			117	0.05 7.78	$\delta_{N2C1C11(14)} + \delta_{N5C1C11(14)} + \delta_{N21C20C17(14)} + \delta_{N24C20C17(14)}$
77	B_1			88	0.15 0.58	$\Gamma_{C17C14C11C1(11)} + \Gamma_{C20C17C14C11(11)}$
78	A_2			57	0 31.82	$\Gamma_{CNCC(11)} + \Gamma_{CCCN\ (10)} + \Gamma_{HCCC\ (10)} + \Gamma_{CCCC\ (14)} + \Gamma_{CCCH\ (11)}$
79	A_1			38	0.15 0.05	$\delta_{C14C11C1(17)} + \delta_{C17C14C11(17)} + \delta_{C20C17C14(17)}$
80	B_1			16	0.36 0.51	$\Gamma_{C14C11C1N5(17)} + \Gamma_{N21C20C17C14(17)}$
81	A_2			14	0 100	$\Gamma_{C14C11C1N2(10)} + \Gamma_{N24C20C17C14(10)}$

ν—stretching, δ—in-plan bending, Γ—out-of plan bending.
s—strong, m—medium, w—weak, v—very.
[a] Scaled wavenumbers calculated at B3LYP/6-311++G(d, p) using scaling factors 0.967.
[b] Relative absorption intensities normalized with highest peak absorption equal to 100.
[c] Relative Raman intensities normalized to 100.
[d] Total energy distribution calculated B3LYP 6-311++G(d,p) level, TED less than 10% are not shown.

electron acceptor represents the ability to obtain an electron. According to the Koopman theorem, the energies of LUMO and HOMO can be described to a good approximation as [47]:

$$\chi \cong -1/2\,(E_{HOMO} + E_{LUMO});\ 2.536\ eV \quad (3)$$

$$\eta \cong -1/2(E_{HOMO} - E_{LUMO});\ 1.901\ eV \quad (4)$$

Several important molecular properties such as chemical hardness (η) and electronegativity (χ) have been defined based on density functional theory [48–50]. Chemical hardness has been used as a tool to understand the chemical reactivity and some other properties of a

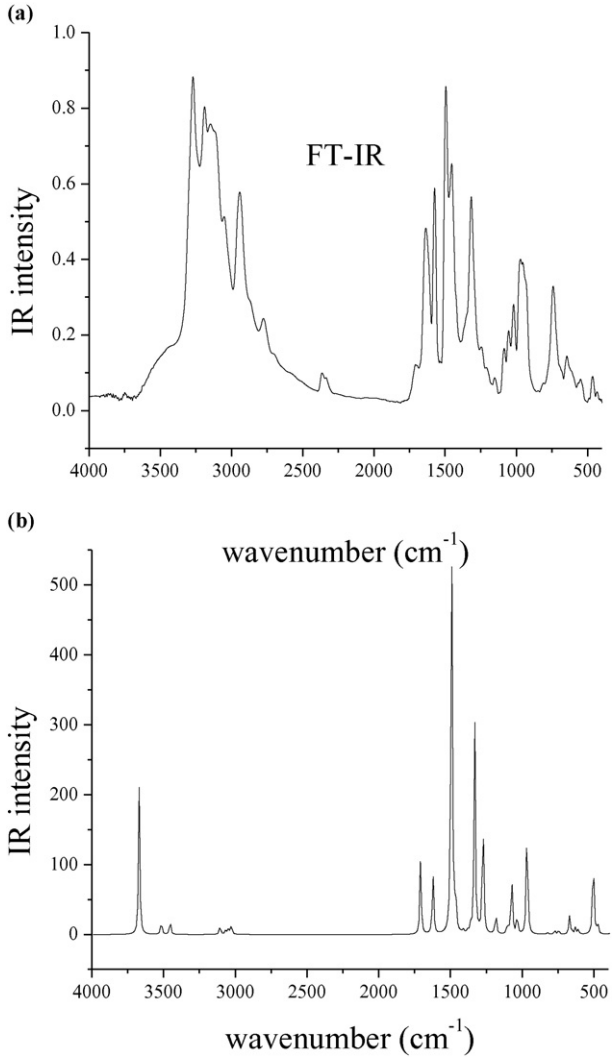

Fig. 2. The experimental (a) and theoretical (b) spectra of BAMTP.

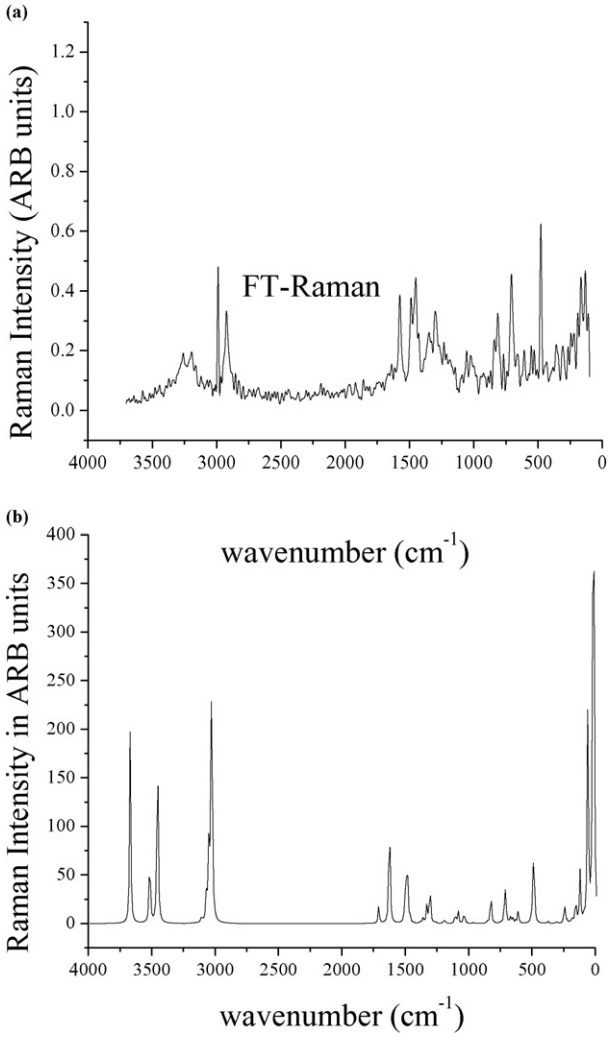

Fig. 3. The experimental (a) and theoretical (b) spectra of BAMTP.

Table 4
The natural bond orbital analysis of BAMTP using B3LYP/6-311++G(d, p) level.

Donor (i)	ED/e	Acceptor (j)	ED/e	[a]$E^{(2)}$ kJ/mol
LPN5	1.60	C_1–N_2(2)	0.02	43.82
		C_3–S_{10}	0.57	60.99
LPN6	1.61	C_1–N_2(2)	0.30	23.1
		C_3–S_{10}	0.57	74.4
LPS10(2)	1.86	C_3–N_5	0.10	14.46
		C_3–N_6	0.07	12.64
LPN21	1.60	C_{20}–N_{24}(2)	0.30	43.82
		C_{22}–S_{29}	0.60	60.99
LPN25	1.61	C_{20}–N_{24}(2)	0.30	23.1
		C_{22}–S_{29}	0.57	74.4
LPS29 (2)	1.86	N_{21}–C_{22}	0.10	14.46
		C_{22}–N_{25}	0.07	12.64

[a] $E^{(2)}$ means energy of hyper conjugative interaction (stabilization energy).

Table 5
Orbital occupancies of BAMTP.

Atoms	1s, 2s, 3s (occupancy)	$2p_x$, $2p_y$, $2p_z$ (occupancy)	dxy, dxz, dyz, dx2y2, dz2
C3	0.9995, 0.48208	0.4495, 0.4633, 0.4449	Vacant
S10	1.0000, 0.9998, 0.9084	0.9998, 0.9998, 0.9998	Vacant

molecular system [51]. It has also been shown that the stability of molecules is related to their chemical hardness [52]. The concept of electronegativity has been introduced as the power of an atom in a molecule to attract electrons onto it [53]. Chemical hardness (η), and electronegativity (χ) are defined in Eqs. (3–4). The calculated chemical hardness is about 2.536 eV, and electronegativity is about 1.901 eV. As a result, when the band gap is large the stability of molecule increases and reactivity decreases [54]. In the present compound, molecular orbitals (MOs) such as alpha (α) and beta (β) are calculated, in which the MO 72 is shown to be the highest occupied level (HOMO) of α MO and its counterpart is shown to be 73 as vacant as LUMO (α*) orbital;besides these, HOMO of β is shown to 70th orbital, in which

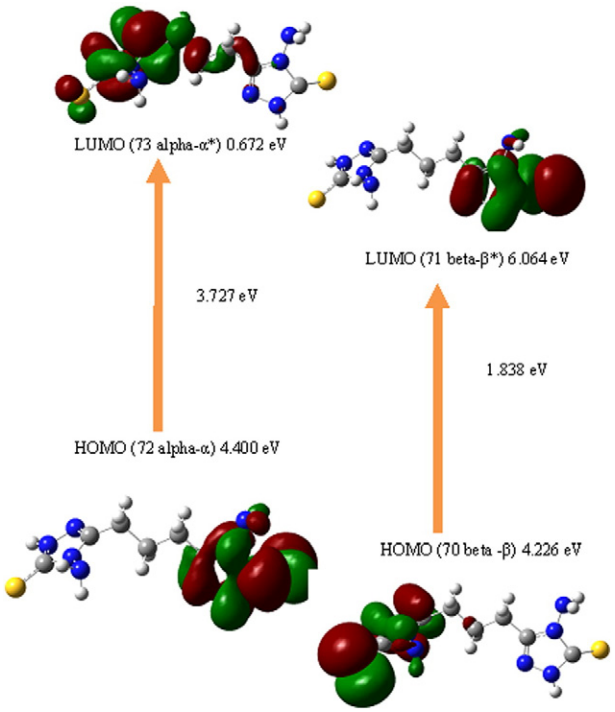

Fig. 4. The frontier molecular α → α* and β → β* orbitals of BAMTP.

the orbitals 71 and 72 became vacant. Since, α MOs are essential, the band gap is measured between MOs 72 (HOMO) and 73 (LUMO); it is about 3.7273 eV. Such a lesser band gap leads the BAMTP molecule as highly reactive. Moreover, the -HOMO is located over the right side triazole ring and sulfur atom, the rest of the part α*-LUMO. Similarly, the molecule has highlighted for β-HOMO and β*-LUMO but essentially the methylene chain is not involved in either MO.

The charge distribution of the molecule has calculated on the basis of Mullikan charge using B3LYP/6-311++G(d,p) level calculation. This calculation depicts the charges of every atom in the molecule. In the present investigation, the negative charge appeared in sulfur (S10, S29 = −0.731), carbon (C11 = −0.633) and nitrogen (N24 = −0.206) atoms. On comparison of atomic charges of C1 and N2, it appears as positive (0.310) and negative (−0.206) charges respectively, whereas the N5 appears about −0.036 a.u. This evidently reveals that the formation of π bond orbital develops the reactive path than the σ bond in the molecule. Based on the atomic charges, graphs were plotted which are shown in Fig. S1 (Supporting information) and the charges are listed in Table S1 (Supporting information).

5. Conclusion

The FT-IR and FT-Raman spectra of BAMTP were recorded and analyzed, most of the recorded vibrational wavenumbers were close to computed wavenumbers. The computed bond lengths were inversely proportional to the bond order. The influence of 2*p*, 3*p* and 3*d* orbitals of nitrogen and sulfur atoms is less at the ground state molecule; $3d^0$ orbital of sulfur became vacant. Since the sulfur contains vacant *d*-orbital in their valence shell, unpairing of *s*- and *p*-electron by promoting them to vacant *d*-orbital is possible. The presence of π bond shows that the molecule possesses more hyperconjugation interaction energy. The energy gap between the highest filled α and unfilled α^* orbitals was determined at 3.727 eV (332.66 nm), which shows that more electron density is in α MOs. Such lesser band gap energy will lead this molecule to become highly reactive and hence, this molecule can be utilized in dye-sensitized solar cells to enhance the performance since analogous triazole band gap is a comparable one (~308 nm).

Supplementary data to this article can be found online at http://dx.doi.org/10.1016/j.saa.2015.12.005.

References

[1] M. Morisue, S. Yamatsu, N. Haruta, Y. Kobuke, Chem. Eur. J. 11 (2005) 5563–5574.
[2] P. Chen, J.H. Yum, F. De Angelis, E. Mosconi, S. Fantacci, S. Moon, R.H. Baker, J. Ko, M.K. Nazeeruddin, M. Gratzel, Nano Lett. 9 (2009) 2487–2492.
[3] X. Zhang, Y. Cui, R. Katoh, N. Koumura, K. Hara, J. Phys. Chem. C 114 (2010) 18283–18290.
[4] H. Kusama, H. Orita, H. Sugihara, Langmuir 24 (2008) 4411–4419.
[5] P. Rajakumar, S. Raja, C. Satheeshkumar, S. Ganesan, P. Maruthamuthu, S.A. Suthanthiraraj, New J. Chem. 34 (2010) 2247–2253.
[6] S. Raja, C. Satheeshkumar, P. Rajakumar, S. Ganesan, P. Maruthamuthu, J. Mater. Chem. 21 (2011) 7700–7704.
[7] P. Rajakumar, C. Satheeshkumar, M. Ravivarma, S. Ganesan, P. Maruthamuthu, J. Mater. Chem. A, (Article in press).
[8] A.E. Stoyanova, S.D. Peyerimhoff, Electrochim. Acta 47 (2002) 1365–1371.
[9] L.M.R. Valdez, A.M. Villafane, D.G. Mitnik, J. Mol. Struct. (THEOCHEM) 716 (2005) 561.
[10] B. Gomez, N.V. Likhanova, M.A.D. Aguilar, R.M. Palou, A. Vela, J.L. Gazquez, J. Phy. Chem. B 110 (2006) 8928–8934.
[11] M. Finšgar, A. Lesar, A. Kokalj, I. Milošev, Electrochim. Acta 53 (2008) 8287–8297.
[12] B.S. Holla, K.N. Poojary, B. Kalluraya, P.V. Gowda, Farmaco 51 (1996) 793–799.
[13] S.N. Pandeya, D. Sriram, G. Nath, E. De Clercq, Arzneim.-Forsch. 50 (2000) 249–255.
[14] F.P. Invidiata, S. Grimaudo, P. Giammanco, L. Giammanco, Farmaco 46 (1991) 1489–1495.
[15] O.G. Todoulou, A.E. Papadaki-Valiraki, E.C. Filippatos, S. Ikeda, E. De Clercq, Eur. J. Med. Chem. 29 (1994) 127–131.
[16] F.P. Invidiata, D. Simoni, F. Scintu, N. Pinna, Farmaco 51 (1996) 659–664.
[17] G.G. Mohamed, C.M. Sharaby, Spectrochim. Acta A 66 (2007) 949–958.
[18] K. Singh, M.S. Barwa, P. Tyagi, Eur. J. Med. Chem. 42 (2007) 394–402.
[19] N.L. Dias Filho, R.M. Costa, F. Marangoni, D. Souza Pereira, J. Colloid Interface, Sci. 316 (2007) 250–259.
[20] Gaussian 03 program, (Gaussian Inc., Walling ford CT) 2004.
[21] H.B. Schlegel, J. Comput. Chem. 3 (1982) 214–218.

[22] A. Frisch, A.B. Nielson, A.J. Holder, Gaussview User Manual, 48, Gaussian Inc., Pittsburgh PA, 2000 4290–4293.
[23] D. Michalska, Raint Program, Wroclaw University of Technology, 2003.
[24] D. Michalska, R. Wysokinski, Chem. Phys. Lett. 403 (2005) 211–217.
[25] S. Prakash, G.D. Tuli, S.K. Babu, R.D. Madan, Adv. Inorg. Chem. 1 (2005) 377–382 19th edition.
[26] J. Baker, A.A. Jarzecki, P. Pulay, J. Phys. Chem. 102A (1998) 1412–1424.
[27] G. Rauhut, P. Pulay, J. Phys. Chem. 99 (1995) 3093–3100.
[28] D. Vedal, O.H. Ellestad, P. Klaboe, Spectrochim. Acta A32 (877) (1976) 877–890.
[29] K. Serbest, A. Ozen, Y. Unver, M. Er, I. Degirmencioglu, K. Sancak, J. Mol. Struct. 922 (2009) 1–10.
[30] K. Druzbicki, E. Mikuli, M.D. Ossowska-Chrusciel, Vib. Spectrosc. 52 (2010) 54–62.
[31] I. Matulkov, I. Nermec, K. Teubuer, P. Nemec, Z. Micka, J. Mol. Struct. 873 (2008) 46–60.
[32] E. Tasal, I. Sidir, Y. Gulseven, C. Ogretir, T. Önkol, J. Mol. Struct. 923 (2009) 141–152.
[33] O. Derel, S. Sudha, N. Sundraganesan, J. Mol. Struct. 994 (2011) 379–386.
[34] A. Dhandapani, S. Manivarman, S. Subashchandrabose, H. Saleem, J. Mol. Struct. 1058 (2014) 41–50.
[35] S. Subashchandrabose, N.R. Babu, H. Saleem, M.S.A. Padusha, J. Mol. Struct. 1094 (2015) 254–263.
[36] T. Karakurt, M. Dincer, A. Cetin, M. Sekerci, Spectrochim. Acta A 77 (2010) 189–198.
[37] S. Subashchandrabose, A.R. Krishnan, H. Saleem, V. Thanikachalam, G. Manikandan, Y. Erdogdu, J. Mol. Struct. 981 (2010) 59–70.
[38] G. Socrates, Infrared, Raman characteristic group frequencies, Tables and Charts, third ed.Wiley, Chichester, 2001.
[39] N. Sundraganesan, S. Kalaichelvan, C. Meganathan, B.D. Joushaua, J. Cornad, Spectrochim. Acta A 71 (2008) 898–906.
[40] M. Silverstein, G.C. Basselar, C. Morill, Spectrometric Identification of Organic Compounds, Wiley, New York, 1981.
[41] L.J. Bellamy, In Infrared Spectra of Complex Molecules, Champman and Hall, London, 1975.
[42] C.N.R. Rao, Chemical Applications of Infrared Spectroscopy, Academic Press, New York, 1963.
[43] C. James, A. AmalRaj, R. Reghunathan, I. Hubert Joe, V.S. Jayakumar, J. Raman Spectrosc. 37 (2006) 1381–1392.
[44] J.N. Lin, Z.R. Chen, S.F. Yuan, J. Zhejiang Univ. Sci. B6 (2005) 584–589.
[45] M. Snehalatha, C. Ravikumar, I. Hubert Joe, N. Sekar, V.S. Jayakumar, Spectrochim. Acta A 72 (2009) 654–662.
[46] A.E. Reed, L.A. Curtics, F. Weinhold, Chem. Rev. 88 (1988) 899–926.
[47] X.-P. Chen, Y.-Q. Ding, Q.-W. Teng, Chin. J. Chem. Phys. 21 (2008) 105.
[48] R.G. Parr, R.A. Donnelly, M. Levy, W.E. Palke, J. Chem. Phys. 68 (1978) 3801–3807.
[49] R.G. Parr, R.G. Pearson, J. Am. Chem. Soc. 105 (1983) 7512–7576.
[50] R.G. Parr, L.V. Szentpaly, S. Liu, J. Am. Chem. Soc. 121 (1999) 1922–1924.
[51] R.G. Parr, P.K. Chattaraj, J. Am. Chem. Soc. 113 (1991) 1854–1855.
[52] Z. Zhou, R.G. Parr, J. Am. Chem. Soc. 112 (1990) 5720–5724.
[53] I. Pauling, The Nature of the Chemical Bond, 3rd ed., Cornell
[54] W. Kohn, A.D. Becke, R.G. Parr, J. Phys. Chem. 100 (1996) 12974–12980.